Available at www.sciencedirect.com

ScienceDirect

journal homepage: www.elsevier.com/locate/watres

ELSEVIER

WATER RESEARCH
A Journal of the International Water Association
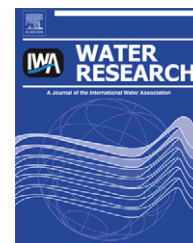
Effects of soluble and particulate substrate on the carbon and energy footprint of wastewater treatment processes

Riccardo Gori [a], Lu-Man Jiang [b], Reza Sobhani [b], Diego Rosso [b,*]

[a] Department of Civil and Environmental Engineering - DICEA, University of Florence, Via S. Marta 3, 50139 Florence, Italy
[b] Department of Civil and Environmental Engineering, University of California, Irvine, CA 92697-2175, USA

ARTICLE INFO

ABSTRACT

Most wastewater treatment plants monitor routinely carbonaceous and nitrogenous load parameters in influent and effluent streams, and often in the intermediate steps. COD fractionation discriminates the selective removal of VSS components in different operations, allowing accurate quantification of the energy requirements and mass flows for secondary treatment, sludge digestion, and sedimentation. We analysed the different effects of COD fractions on carbon and energy footprint in a wastewater treatment plant with activated sludge in nutrient removal mode and anaerobic digestion of the sludge with biogas energy recovery. After presenting a simple rational procedure for COD and solids fractions quantification, we use our carbon and energy footprint models to quantify the effects of varying fractions on carbon equivalent flows, process energy demand and recovery. A full-scale real process was modelled with this procedure and the results are reported in terms of energy and carbon footprint. For a given process, the increase of the ratio sCOD/COD increases the energy demand on the aeration reactors, the associated CO_2 direct emission from respiration, and the indirect emission for power generation. Even though it appears as if enhanced primary sedimentation is a carbon and energy footprint mitigation practice, care must be used since the nutrient removal process downstream may suffer from an excessive bCOD removal and an increased mean cell retention time for nutrient removal may be required.

© 2011 Elsevier Ltd. All rights reserved.

1. Introduction

The need for a rigorous scientific approach to research and model wastewater treatment processes has been paramount to water research for nearly a century: "American sewerage practice is noteworthy among the branches of engineering for the preponderating influence of experience rather than experiment upon the development of many of its features, apart from those concerned with the treatment of sewage" (Metcalf and Eddy, 1914). The qualification of the oxygen demand and suspended solids components is a key step in transcending this practice-based engineering approach.

Modelling biological wastewater treatment processes has been the major driving force for the development of protocols aimed at splitting macroscopic parameters (such as total and volatile suspended solids, TSS and VSS, or biochemical and chemical oxygen demand, BOD_5 and COD) into fractions with different behaviour in the treatment processes. In particular, COD fractionation was introduced as a tool for the evaluation and modelling of biological treatment processes performance (Henze, 1992).

Modelling of activated sludge processes (ASP) is usually carried out with structured models, such as the ASM family (Henze et al., 2000). The ASM1 represents the basic model used

---

Notation

$bCOD_i$	biodegradable COD in flow line i ($mass_{bCOD}$/d)
$bVSS$	biodegradable volatile suspended solids (mg/l)
$bVSS_{PS}$	biodegradable VSS in primary sludge ($mass_{VSS}$/d)
$bVSS_{SS}$	biodegradable VSS in secondary sludge ($mass_{VSS}$/d)
e_D	energy demand (kWh/d)
$e_{D,AD}$	energy demand for anaerobic digestion (kWh/d)
$e_{D,ASP}$	energy demand for activated sludge aeration (kWh/d)
$e_{D,PS}$	energy demand for primary sedimentation (kWh/d)
$e_{D,SS}$	energy demand for secondary sedimentation (kWh/d)
$e_{D,O}$	energy demand for other equipment (kWh/d)
e_R	energy recovery (kWh/d)
f_d	fraction of biomass contributing to biomass debris (−)
h_{BG}	calorific value of the biogas (kJ/kg_{biogas})
$iTSS$	inert total suspended solids ($mass_{TSS}$/l)
k	maximum substrate utilisation rate ($mass_{COD}$/$mass_{VSS}$ d)
$k_{d,A}$	decay rate of autotrophic biomass (1/d)
$k_{d,H}$	decay rate of heterotrophic biomass (1/d)
$k_{d,ANA}$	decay rate of biomass under anaerobic conditions (1/d)
K_s	half-saturation constant (mg/l)
m_{BG}	mass flow of biogas ($mass_{BG}$/d)
$m_{BG,VSS}$	mass flow of biogas calculated from VSS destruction ($mass_{BG}$/d)
$m_{BS,COD}$	mass flow of biosolids as COD ($mass_{COD}$/d)
$m_{BS,bCOD}$	mass flow of biosolids as bCOD ($mass_{COD}$/d)
$m_{BS,VSS}$	mass flow of biosolids calculated from VSS destruction ($mass_{VSS}$/d)
m_{CH_4}	mass flow of methane ($mass_{CH_4}$/d)
$m_{CH_4,fugitive}$	mass flow of methane fugitive emission ($mass_{CH_4}$/d)
$m_{CH_4,dewatering}$	mass flow of methane released during biosolids dewatering ($mass_{CH_4}$/d)
$m_{CO_2,ASP}$	mass flow of CO_2 in the activated sludge off-gas ($mass_{CO_2}$/d)
$m_{CO_2,AD}$	mass flow of CO_2 in the biogas ($mass_{CO_2}$/d)
m_{CO_2eq}	total mass flow of CO_{2eq} ($mass_{CO_2}$/d)
m_{CO_2,CH_4comb}	mass flow of CO_2 due to methane combustion ($mass_{CO_2}$/d)
$m_{CO_2eq,PG}$	mass flow of CO_2 due to off-site power generation ($mass_{CO_2}$/d)
$m_{CO_2eq,offset}$	mass flow of $CO_{2,eq}$ offset due to energy recovery ($mass_{CO_2}$/d)
$m_{CO_2eq,fugitive}$	mass flow of $CO_{2,eq}$ due to fugitive emission ($mass_{CO_2}$/d)
$m_{DIG,in}$	mass flow entering the digester ($mass_{bCOD}$/d)
$m_{PS,bCOD}$	bCOD mass flow of waste primary sludge ($mass_{bCOD}$/d)
$m_{PS,COD}$	COD mass flow of waste primary sludge ($mass_{COD}$/d)
$m_{PS,VSS}$	COD mass flow of waste primary sludge ($mass_{VSS}$/d)
$m_{PS,TSS}$	COD mass flow of waste primary sludge ($mass_{TSS}$/d)

m_{SS}	mass flow of waste secondary sludge ($mass_{bCOD}$/d)
$m_{bCOD-CH4}$	bCOD converted in methane in the anaerobic digester ($mass_{bCOD}$/d)
$m_{bCOD-ANA\ biomass}$	bCOD converted in biomass under anaerobic conditions ($mass_{bCOD}$/d)
$m_{bCOD-SN}$	bCOD in the supernatant line ($mass_{bCOD}$/d)
$m_{bCOD-sol}$	bCOD solubilised in the anaerobic digester ($mass_{bCOD}$/d)
MCRT	mean cell retention time (d)
NO_x	concentration of oxidised nitrogen (mg_N/l)
$pbCOD_i$	particulate biodegradable COD in flow line i (mg/l)
$pnbCOD_i$	particulate non-biodegradable COD in flow line i (mg/l)
$P_{x,active\ bio}$	daily active biomass production ($mass_{VSS}$/d)
$P_{x,VSS}$	daily excess sludge production in terms of VSS ($mass_{VSS}$/d)
$P_{x,TSS}$	daily total excess sludge production ($mass_{TSS}$/d)
$P_{x,COD}$	daily total excess sludge production in terms of COD ($mass_{COD}$/d)
$P_{x,ANA}$	biomass production under anaerobic conditions ($mass_{VSS}$/d)
Q	influent flow rate (m^3/d)
Q_{BG}	flow rate of biogas leaving the anaerobic digester (Nm^3/d)
$sbCOD_i$	soluble biodegradable COD in flow line i (mg/l)
$snbCOD_i$	soluble non-biodegradable COD in flow line i (mg/l)
SRT_{DIG}	digester solids retention time (d)
VSS	volatile suspended solids (mg/l)
TSS	total suspended solids (mg/l)
Y_A	autotrophic biomass yield ($mass_{VSS}$/$mass_{N,oxidised}$)
Y_H	heterotrophic biomass yield ($mass_{VSS}$/$mass_{COD}$)
Y_{ANA}	biomass yield in anaerobic conditions ($mass_{VSS}$/$mass_{COD}$)
$\Delta bCOD$	difference between solubilised bCOD in the digester and bCOD in the supernatant line ($mass_{COD}$/d)

Greek letters

β_{CH_4}	specific methane production (Nm^3/kg_{bCOD})
η_{ASP}	bCOD removal in the activated sludge process (%)
η_{DIG}	bCOD solubilised in the digester (%)
$\eta_{DIG,VSS}$	percent VSS destruction in the digester (%)
$\eta_{DIG,TSS}$	percent TSS destruction in the digester (%)
η_{ER}	efficiency of the energy recovery unit (−)
η_{PS}	particulate removal in primary sedimentation (%)
η_{FE}	fugitive emission of methane (%)
$\kappa_{BIOMASS}$	carbon emission intensity of biomass (kg_{CO_2eq}/kg_{COD})
κ_{COD}	carbon emission intensity of COD (kg_{CO_2eq}/kg_{COD})
κ_{PG}	specific CO_2 emission for off-site energy generation (kg_{CO_2eq}/kWh)
ρ_{CH_4}	methane density (kg_{CH_4}/Nm^3)
ρ_{BG}	biogas density (kg_{BG}/Nm^3)
ρ_{CO_2}	CO_2 density (kg_{CO_2}/Nm^3)

Subscripts

i	primary influent (PI); primary effluent (PE); secondary effluent (SE)

to describe removal of organic carbon and nitrogen, consumption of nitrate and oxygen as electron acceptors, and sludge production (Henze et al., 1987). Nowadays, the ASM1 model is still often the state-of-the-art for modelling activated sludge systems (Roeleveld and van Loosdrecht, 2002). Regardless of the model used, COD and nitrogen have to be fractionated in order to differentiate compounds with different mechanisms and rates of biodegradation, which in turn determine their different fate in sedimentation and biological processes. The basic approach for fractionation relies on considerations over the biodegradability and solubility of wastewaters components.

Several protocols, from simplified and practical to those of increased complexity, were developed for wastewater characterisation: two of the major were developed by STOWA (Hulsbeek et al., 2002) and Biomath (Vanrolleghem et al., 2003). Both of them rely on the combination of biological (respirometric) and physical-chemical measurements which are not widely performed in normal full-scale plant operations.

On a routine basis, most treatment plants monitor COD, BOD$_5$, TKN, NH$_4^+$-N and PO$_4^{3-}$-P in influent and effluent streams, and oftentimes in the intermediate process steps. The typical assumption for municipal wastewater quality is that it has minor or no industrial wastewater contribution. In reality, the composition of municipal wastewater can vary widely from one site to another and in the same location over time. Influent quality is affected by several site-specific conditions, such as the nature of discharged compounds, in-sewer microbial transformation, sewer length and its residence time, gas-transfers in sewers, water and ambient temperatures (Vollertsen et al., 1999). For this reason, the extension of models from one site to another may result in inaccuracies, and the preliminary collection of site-specific data for fractionation is always beneficial.

The introduction of COD fractionation in a mass-balance based model discriminates the selective removal of VSS components, which is key for the accurate quantification of the energy requirements and mass flows for secondary treatment, sludge digestion, and sedimentation. For example, two limit cases could be a treatment plant operating chemically-enhanced primary treatment followed by no biological process, the other operating an activated sludge at low sludge age with inadequate or no primary treatment. A simple rational procedure for the calculation of COD fractions hence pCOD/VSS (such as that reported in the following section), would provide precious information to distinguish the two cases. Even though both plants could be hypothesised to have matching VSS mass flow rates to their digesters, the quality of each VSS stream in terms of pCOD/VSS would be substantially different. Therefore, the two plants would yield different VSS removal and biogas production in their respective digesters. Currently, most of the design procedures widely taught in textbooks rely on few empirical data (inter alia, Metcalf and Eddy, 2003). Due to the lack of published experimental data and to the range of possible COD fractions, there is a need for the quantification of the effects of pCOD/VSS variations.

Presently, the reduction of carbon and energy footprint (CFP and eFP, respectively) is a worldwide concern associated with global warming mitigation and adaptation strategies. Treatment utilities can play a significantly beneficial role here

because of the large amounts of carbonaceous organic matter processed daily. This COD may be converted to biomass and CO$_2$, and ultimately utilised for energy recovery and/or carbon sequestration (Rosso and Stenstrom, 2008). However, the removal of COD from the water stream is energy intensive and is associated with direct and indirect release of greenhouse gases (Monteith et al., 2005; de Haas et al., 2008; Park et al., 2010; Ahn et al., 2010; Foley et al., 2010), which may have a relevant weight on process CFP (Rosso et al., 2009). Regardless of the anthropogenic or biogenic nature of the COD in the influent wastewater, the treatment process can add the mitigation of greenhouse gas emissions to its already evident public and environmental health benefits.

The goal of this paper is to show the effect of varying COD and solids fractions on process carbon and energy footprints. After presenting a simple rational procedure for COD and solids fractions quantification, we use our carbon and energy footprint models to quantify the effects of varying fractions on carbon equivalent flows, process energy demand and recovery. This model does not aim at replacing the detailed structured models already available (e.g. ASM, ADM), but rather at introducing a more rigorous approach to the mass-balance based carbon and energy footprint analysis based on a simplified set of process input data.

2. Materials and methods

2.1. Plant data selection

We selected a municipal water reclamation plant ($Q \sim 60000$ m^3 d^{-1}) located in the United States in a warm area ($T_{ww,avg} = 20$ °C) with process schematic matching that of Fig. 1, with the addition of headworks and disinfection. The main process parameters were collected and are reported in Table 1. Data sets were collected as daily measurements for 2010, and were processed with the COD fractionation procedure described below to quantify yearly averages of COD fractions for variable pCOD/VSS ratio. Also, the energy consumption per unit operation was collected from plant data logs, confirming that aeration energy was the dominant process energy component (64.0–74.2% of the total process energy), with the exclusion of effluent pumping. We must specify here that the sludge processing (i.e., thickening, mesophilic anaerobic digestion, dewatering and disposal) and the biogas energy recovery are performed off-site at a larger centralised facility. Therefore, the energy recovery data for this plant cannot be retrieved directly and can only be estimated using this model.

2.2. Procedure to derive COD and TSS fractions

Starting from the typical data available for any plant (COD, BOD$_5$, TSS and VSS), COD fractions, and TSS fractions in primary influent (PI) and primary effluent (PE) can be calculated from a mass balance on the primary settling tank. The estimation of pCOD/VSS for biodegradable and non-biodegradable particulate organics requires advanced measurements never performed during plant operations, and typically belonging to the research domain. One assumption is

Fig. 1 – Wastewater treatment plant layout and depiction of COD and energy flows. All symbols are defined in the paper notation.

considering the non-biodegradable fraction of the sCOD (i.e., the snbCOD) as conservative and equal to the filtered secondary effluent COD. This is acceptable when the plant is operated at an MCRT sufficiently high to remove the sbCOD to

Table 1 – **Summary of process characteristics for the plant considered here.**

Parameter	Value
Flow rate (AVG, m^3/d)	60000
T_W (AVG, °C)	20
Activated sludge mean cell retention time (AVG, d)	8.5
Digester sludge retention time (AVG, d)	30
Influent	
COD_{in} (mg/l)	541 ± 100
$BOD_{5,in}$ (mg/l)	243 ± 48
TSS_{in} (mg/l)	308 ± 56
VSS_{in} (mg/l)	263 ± 50
$NH_4–N_{in}$ (mg/l)	N/A
Primary effluent	
COD_{PI} (mg/l)	284 ± 54
BOD_{5PI} (mg/l)	144 ± 36
TSS_{PI} (mg/l)	104 ± 31
VSS_{PI} (mg/l)	87 ± 27
NH_4-N_{PI} (mg/l)	28 ± 3.8
Secondary effluent	
COD_{SE} (mg/l)	27 ± 7.1
BOD_{5SE} (mg/l)	7.1 ± 2.9
TSS_{SE} (mg/l)	13 ± 5.3
VSS_{SE} (mg/l)	10 ± 4.2
$NH_4–N_{SE}$ (mg/l)	0.13 ± 0.2
Filtered secondary effluent	
COD_{fe} (mg/l)	18 ± 4.1
$BOD_{5,fe}$ (mg/l)	1,8 ± 0.9
TSS_{fe} (mg/l)	1.0 ± 0.5

the highest extent. This approach has been used in previous works (e.g., Ekama, 2009; Takacs and Vanrolleghem, 2006) and is widely accepted in modelling.

Also, the concentration of pCOD and VSS varies over the diurnal cycle. With our approach, we assume that all particulate materials, regardless of their biodegradability, are characterised by the same value of pCOD/VSS. This implies that the wastewater is uniform, i.e. the differential ratio of its components (lipids, carbohydrates, proteins, etc.) does not change with time. The calculations used to derive COD and TSS fractions are summarised in Table 2.

2.3. Carbon and energy footprint models as function of COD fractions

The CFP and eFP models are an evolution of previously published methodologies (Monteith et al., 2005; Rosso and Stenstrom, 2008). In this paper the model was applied to the process illustrated in Fig. 1. This process was selected since it is the most common scenario for a wastewater treatment plant layout worldwide. Fig. 1 illustrates the units included in this model, and summarises the mass flows amongst the biological and settling units. The expression of all mass in COD units allows us to express all the mass flows throughout the plant in terms of bCOD. In our approach, there is no difference in the transformation of primary and secondary sludge in terms of bCOD. That would not be true in terms of VSS, i.e. the primary sludge VSS destruction is expected to be far higher than secondary sludge for municipal wastewater. As usual with CFP and eFP models, several assumptions must be taken. Caution must be used when applying the model to other plants. The main assumptions taken in our work are summarised in Table 3.

Table 2 – Procedure for the estimation of COD and TSS fractions as calculated from commonly measured parameters.

Parameter	Symbol	ASM symbol	Formula
Particulate COD	pCOD	–	pCOD/VSS - VSS
Soluble COD	sCOD	–	COD - pCOD
Biodegradable COD	bCOD	–	1,6 - BOD$_5$
Soluble non-biodegradable COD	snbCOD	S_I[a]	soluble COD of filtered SE
Soluble biodegradable COD	sbCOD	S_S	sCOD - S_I
Particulate biodegradable COD	pbCOD	X_S	bCOD - S_S
Particulate non-biodegradable COD	pnbCOD	X_I[a]	pCOD - X_S
Non-biodegradable VSS	nbVSS	–	pCOD/VSS - X_I
Biodegradable VSS	bVSS	–	pCOD/VSS - X_S
Inert TSS	iTSS	–	TSS - VSS

a Conservative fractions.

2.3.1. Mass flow modelling for primary treatment

For the following mass flow analysis we express all mass flows with units of mass$_j$/d, where j is any of the pertinent subscripts. For each mass flow equation, appropriate conversion factors are required, depending of the actual units desired (SI, USCS, technical metric units, etc.).

The mass flow in and out of primary sedimentation is the product of primary influent and effluent concentrations and the flow rate. For each of the COD fractions a balance can be written between primary influent (PI) and effluent (PE):

$$sbCOD_{PE} = sbCOD_{PI} \tag{1}$$

$$snbCOD_{PE} = snbCOD_{PI} \tag{2}$$

$$pbCOD_{PE} = pbCOD_{PI}(1 - \eta_{PS}) \tag{3}$$

$$pnbCOD_{PE} = pnbCOD_{PI}(1 - \eta_{PS}) \tag{4}$$

where, sbCOD$_i$ = soluble biodegradable COD (mg/l)
   snbCOD$_i$ = soluble non-biodegradable COD (mg/l)
   pbCOD$_i$ = particulate biodegradable COD (mg/l)
   pnbCOD$_i$ = particulate non-biodegradable COD (mg/l)
   i = primary influent (PI) or primary effluent (PE)
   and the sedimentation efficiency of the primary settler (η_{PS}; %) is

$$\eta_{PS} = 100 \cdot \left[1 - \frac{pCOD_{PE}}{pCOD_{PI}}\right] = 100 \cdot \left[1 - \frac{(pbCOD_{PE} + pnbCOD_{PE})}{(pbCOD_{PI} + pnbCOD_{PI})}\right] \tag{5}$$

The mass flow of primary waste sludge in terms of COD and bCOD as well as VSS and TSS (m_{PS}; mass$_{COD}$/d, mass$_{bCOD}$/d, mass$_{VSS}$/d, mass$_{TSS}$/d respectively), leaving the sedimentation basin are:

$$m_{PS,bCOD} = Q \cdot pbCOD_{PI} \cdot \eta_{PS} \tag{6}$$

$$m_{PS,COD} = Q \cdot pCOD_{PI} \cdot \eta_{PS} \tag{7}$$

$$m_{PS,VSS} = Q \cdot VSS_{PI} \cdot \eta_{PS} \tag{8}$$

$$m_{PS,TSS} = Q \cdot TSS_{PI} \cdot \eta_{PS} \tag{9}$$

where
   Q = plant influent flow rate (m^3/d)
   and

$$pCOD_{PI} = pbCOD_{PI} + pnbCOD_{PI} \tag{10}$$

is the total particulate COD in the primary influent (mg/l). The value of η_{PS} is a key parameter defining the energy performance of the overall process, and it will be discussed below.

2.3.2. Mass flow modelling for secondary treatment

These flows derived from mass balance analysis analogous to the ASM1 approach with mean cell retention time (MCRT) sufficiently long to ensure complete hydrolysis of pbCOD (Henze et al., 2000). This assumption implies that the bCOD in the secondary effluent is all soluble (i.e., sbCOD), with exception of a negligible contribution of particulate from microorganisms being washed out of the secondary clarifier. Based on the mass balance analysis of a well-mixed activated sludge reactor (Metcalf and Eddy, 2003), the concentrations of COD fractions (mg/l) in the secondary effluent are:

$$bCOD_{SE} \simeq sbCOD_{SE} = \frac{K_S[1 + (k_{d,H})MCRT]}{MCRT(Y_H k - k_{d,H}) - 1} \tag{11}$$

$$snbCOD_{SE} = snbCOD_{PE} \tag{12}$$

$$COD_{SE} = snbCOD_{PE} + bCOD_{SE} \tag{13}$$

where K_s = half-saturation constant (mg/l)
   $k_{d,H}$ = decay rate of heterotrophic biomass (1/d)
   Y_H = heterotrophic biomass yield (mass$_{VSS}$/mass$_{COD}$)
   k = maximum substrate utilisation rate (mass$_{COD}$/mass$_{VSS}$ d)
   MCRT = mean cell retention time (d).
   The oxidation of biodegradable COD and ammonia results in a daily active biomass production $P_{x,active bio}$ (mass$_{VSS}$/d):

$$P_{x,active\,bio} = \frac{Q \cdot Y_H \cdot \eta_{ASP} \cdot bCOD_{PE}}{1 + (k_{d,H}) \cdot MCRT} + \frac{Q \cdot Y_A \cdot NO_x}{1 + (k_{d,A}) \cdot MCRT} \tag{14}$$

where
   Q = flow rate through the activated sludge process (m^3/d)
   $k_{d,A}$ = decay rate of autotrophic biomass (1/d)
   Y_A = autotrophic biomass yield (mass$_{VSS}$/mass$_{N,oxidized}$)
   NO$_x$ = concentration of oxidised nitrogen (mg$_N$/l)
   and with the bCOD removal in the activated sludge reactor η_{ASP} (%) calculated from Eqs. (1), (2), and (11):

$$\eta_{ASP} = 100 \cdot \left[1 - \frac{bCOD_{SE}}{bCOD_{PE}}\right]$$
$$= 100 \cdot \left\{1 - \frac{K_S[1 + (k_{d,H})MCRT]/[MCRT(Y_H k - k_{d,H}) - 1]}{(sbCOD_{PE} + pbCOD_{PE})}\right\} \tag{15}$$

Consequently, the mass flow of secondary sludge in terms of bCOD from the sludge wasting line m_{SS} (mass$_{bCOD}$/d) is:

$$m_{SS} = 1.42 \cdot P_x \cdot (1 - f_d) \tag{16}$$

where
   f_d = fraction of biomass contributing to biomass debris (–).
   Similarly to the approach used in ASM1 and according to Grady et al. (1998), we assumed that f_d represents the fraction

Table 3 – Main assumptions made for calculation of carbon and energy footprint.	
Process section	Assumptions
Influent quality	Selected according to data from WWTP (Table 1)
Primary sedimentation	VSS and TSS removal efficiency = 66%
	COD removal efficiency = 35–54% (calculated on the basis of VSS efficiency removal and pCOD/VSS ratio between 1.07 and 1.87)
Activated sludge	Kinetic and stoichiometric parameters for heterotrophic bacteria @20 °C: maximum growth rate (μ): 6 d^{-1}
	Half-saturation constant: 20 g bCOD/m^3
	Yield (Y_H): 0.67 gCOD/gCOD
	Net decay rate k_d: 0.12 d^{-1}
	Fraction of biomass contributing to biomass debris (f_d): 0.15
	Kinetic and stoichiometric parameters for autotrophic bacteria @20 °C: maximum growth rate (μ_N): 0.5 d^{-1}
	Half-saturation constant: 0.5 g NH_4^+–N/m^3
	Yield (Y_N): 0.12 gVSS/g NH_4^+-N
	Net decay rate k_{dN}: 0.12 d^{-1}
	Arrhenius constants for correction of kinetic parameters with temperature: 1.07 for maximum growth rate, 1.04 for net decay rate
	MCRT = 10 d
	Dissolved oxygen = 2 mg/l
	Kinetic and stoichiometric parameters were assumed from Metcalf and Eddy (2003)
	Fine pore aeration with αSOTE[a] = 15%
Anaerobic digestion	bCOD solubilised = 85%
	Biogas: 65% methane and 35% CO_2
	Methane production: 0.35 Nm^3/kg $_{bCOD,rem}$
	Methane fugitive emission: 2%
	VSS reduction calculated according to pCOD/VSS values
	Biomass production calculated according to Metcalf and Eddy (2003)
	bCOD in supernatant line returned to the headworks assumed as 3% of solubilised bCOD
	Y_{ANA} = 0.08 gVSS/gCOD
	$k_{d,ANA}$ = 0.03 d^{-1}
	SRT_{dig} = 30 d
Dewatering section (belt-press)	Dry matter in influent biosolids[a]: 2.1%
	Dry matter in dewatered sludge[a]: 19.2%
Energy consumption and recovery	Specific energy consumption[a] (kWh/m^3$_{treated\ in\ the\ section}$):
	0.026 for influent pumping, 0.007 for preliminary treatments, 0.032 for primary settling tank, 0.024 for secondary settling tank, 2.116 for sludge dewatering, 0.16 kWh/kg dry solids fed to the anaerobic digesters
	Efficiency of energy recovery from methane combustion: 50%
	Methane specific energy: 35.80 MJ/m^3
Emission for off-site electricity generation	Specific CO_{2eq} emission for electricity generation and for calculation of CO_{2eq} offset from biogas combustion: 0.245 kg CO_{2eq}/kWh[b]

a Actual data at the WWTP modelled.
b From EIA (2009).

of biomass that can be considered not biodegradable. The conversion factor 1.42 is required to express the mass of microbial VSS in COD units, assuming the generally acknowledged empirical formula $C_5H_7NO_2$ for bacterial biomass (Metcalf and Eddy, 2003).

In order to complete the analysis of energy and carbon footprint for the whole process, the total excess sludge production from ASP both in terms of VSS mass and COD must be calculated. The calculation of total excess sludge production is based on the mass balance analysis of both endogenous and exogenous biodegradable and non-biodegradable fractions as well as the inert suspended solids in a well-mixed activated sludge reactor. The typical assumption (Metcalf and Eddy, 2003) is that both the pnbCOD and the inert total suspended solids (iTSS, mg/l) not removed in primary sedimentation are embedded in the activated sludge flocs. Using this hypothesis, the daily excess sludge production $P_{x,VSS}$

(mass$_{VSS}$/d), $P_{x,TSS}$ (mass$_{TSS}$/d), and $P_{x,COD}$ (mass$_{COD}$/d) can be calculated as follows:

$$P_{x,VSS} = \frac{P_{x,active\ bio}}{0.85} + \frac{1}{0.85} \frac{f_d \cdot k_{d,H} \cdot Q \cdot Y_H \cdot MCRT}{1 + k_{d,H} \cdot MCRT} + Q \cdot nbVSS_{PE} \quad (17)$$

$$P_{x,TSS} = \frac{P_{x,active\ bio}}{0.85} + \frac{1}{0.85} \frac{f_d \cdot k_{d,H} \cdot Q \cdot Y_H \cdot MCRT}{1 + k_{d,H} \cdot MCRT} + Q \cdot nbVSS_{PE} + Q \cdot iTSS_{PE} \quad (18)$$

$$P_{x,COD} = \left(P_{x,active\ bio} + \frac{f_d \cdot k_{d,H} \cdot Q \cdot Y_H \cdot MCRT}{1 + k_{d,H} \cdot MCRT} \right) \cdot 1.42 + Q \cdot nbVSS_{PE} \cdot pCOD/VSS \quad (19)$$

2.3.3. Mass flow modelling for sludge digestion
In our approach we assumed a value for bCOD transformation in the digester (η_{DIG}) and CH$_4$ and CO$_2$ production were

estimated performing a bCOD mass balance analysis on the digester (summarised in Fig. 1). The influent mass flow of bCOD to the digester $m_{\text{DIG,in}}$ ($\text{mass}_{\text{bCOD}}$/d) can be calculated from the sum of Eqs. (6) and (16):

$$m_{\text{DIG,in}} = m_{\text{PS,bCOD}} + m_{\text{SS}} = Q \cdot \text{pCOD}_{\text{PI}} \cdot \eta_{\text{PS}} + 1.42 P_{\text{x,active bio}} \cdot (1 - f_{\text{d}}) \tag{20}$$

Assuming that a fraction of digester's influent bCOD solubilises and that of the solubilised bCOD a fraction leaves as sbCOD in the supernatant line and a fraction is converted to anaerobic biomass, the bCOD mass flow in biogas can be calculated as:

$$\begin{Bmatrix} m_{\text{bCOD}-\text{CH}_4} \\ \text{bCOD} \\ \text{transformed} \\ \text{to biogas} \end{Bmatrix} = \begin{Bmatrix} m_{\text{bCOD}-\text{sol}} \\ \text{bCOD} \\ \text{solubilised} \\ \text{in the digester} \end{Bmatrix} - \begin{Bmatrix} m_{\text{bCOD}-\text{SN}} \\ \text{bCOD} \\ \text{in supernatant} \end{Bmatrix} - \begin{Bmatrix} m_{\text{bCOD}-\text{ANA biomass}} \\ \text{bCOD of anaerobic} \\ \text{biomass produced} \end{Bmatrix}$$
$$= \eta_{\text{DIG}} \cdot \left[Q \cdot \text{pCOD}_{\text{PI}} \cdot \eta_{\text{PS}} + 1.42 \cdot P_{\text{x, active bio}} \cdot (1 - f_{\text{d}}) \right] - m_{\text{bCOD}-\text{SN}} - m_{\text{bCOD}-\text{ANA biomass}} \tag{21}$$

where

η_{DIG} = bCOD solubilised in the digester (%; see Table 3).

In this paper we assumed that 85% of the bCOD in the digester influent is solubilised within the digester (i.e., $\eta_{\text{DIG}} = 0.85$), and that 3% of the solubilised bCOD leaves the digester in the supernatant line ($m_{\text{bCOD,SN}}$). The bCOD converted in biomass under anaerobic conditions is calculated as:

$$P_{\text{x,ANA}} = \frac{Y_{\text{ANA}} \cdot \Delta \text{bCOD}}{1 + (k_{\text{d,ANA}}) \cdot \text{SRT}_{\text{DIG}}} \tag{22}$$

where

Y_{ANA} = biomass yield in anaerobic conditions ($\text{mass}_{\text{VSS}}/\text{mass}_{\text{COD}}$)

SRT_{dig} = digester solid retention time (d)

$P_{\text{x,ANA}}$ = biomass production under anaerobic conditions (mass_{VSS}/d)

ΔbCOD = difference between solubilised bCOD and bCOD in the supernatant line (mass_{COD}/d).

The methane m_{CH_4} (mass_{CH4}/d) and biogas production m_{BG} (mass_{BG}/d) can be calculated using Eq. (21):

$$m_{\text{CH}_4} = m_{\text{bCOD}-\text{CH}_4} \cdot \beta_{\text{CH}_4} \cdot \rho_{\text{CH}_4} \tag{23}$$

$$m_{\text{BG}} = \frac{m_{\text{CH}_4}}{0.65} \frac{\rho_{\text{BG}}}{\rho_{\text{CH}_4}} \tag{24}$$

where

Q_{BG} = flow rate of biogas leaving the anaerobic digester (m^3/d)

β_{CH_4} = specific methane production ($\text{Nm}^3/\text{kg}_{\text{bCOD}}$)

ρ_{CH_4} = methane density ($\text{kg}_{\text{CH}_4}/\text{Nm}^3$)

ρ_{BG} = biogas density ($\text{kg}_{\text{CH}_4}/\text{m}^3$).

Considering that there is no COD destruction in an anaerobic reactor but only COD transformation, and assuming no nitrate or sulphate reduction, we can write:

$$\begin{Bmatrix} \text{Total COD mass} \\ \text{flow in digester inlet} \end{Bmatrix} = \begin{Bmatrix} \text{COD mass flow} \\ \text{in biogas} \end{Bmatrix}$$
$$- \begin{Bmatrix} \text{COD mass flow} \\ \text{in supernatant} \end{Bmatrix} + \begin{Bmatrix} \text{COD mass flow} \\ \text{in biosolids} \end{Bmatrix} \tag{25}$$

From Eq. (25), the biosolids mass flow in terms of both COD ($m_{\text{BS,COD}}$ as mass_{COD}/d) and bCOD ($m_{\text{BS,bCOD}}$ as $\text{mass}_{\text{bCOD}}$/d) are:

$$m_{\text{BS,bCOD}} = \begin{Bmatrix} \text{Total bCOD} \\ \text{in the digester} \\ \text{influent} \end{Bmatrix} - \begin{Bmatrix} \text{COD of} \\ \text{biogas} \\ \text{produced} \end{Bmatrix} - \begin{Bmatrix} \text{COD in} \\ \text{supernatant} \end{Bmatrix} + \begin{Bmatrix} \text{COD of} \\ \text{biomass} \\ \text{produced} \end{Bmatrix}$$
$$= m_{\text{PS,COD}} + P_{\text{x,COD}} + 1.42 \cdot P_{\text{x,ANA}}$$
$$= \left[Q \cdot \text{pCOD}_{\text{PI}} \cdot \eta_{\text{PS}} + 1.42 \cdot P_{\text{x, active bio}} \cdot (1 - f_{\text{d}}) \right] - m_{\text{bCOD}-\text{CH}_4} - m_{\text{bCOD}-\text{SN}} + 1.42 \cdot P_{\text{x,ANA}} \tag{26}$$

COD is conservative and therefore only transformed from influent solids to effluent solids and gas, while VSS is not conservative and is destroyed producing different biogas yield for different types of VSS. Only the VSS portion of the TSS is destroyed whilst the non-volatile remainder is conservative, hence not all TSS are destroyed but are in fact reduced. Therefore, throughout the paper we refer to COD transformation, VSS destruction, and TSS reduction. The percentage reduction in terms of VSS and TSS in the digester can be calculated as follows:

$$\eta_{\text{DIG,VSS}} = \left\{ \eta_{\text{DIG}} \cdot \left[\frac{Q \cdot \text{pCOD}_{\text{PI}} \cdot \eta_{\text{PS}}}{\text{pCOD/VSS}} + P_{\text{x, active bio}} \cdot \left(1 - f_{\text{d}} \right) \right] - 1.42 \cdot P_{\text{x,ANA}} \right\} \cdot \frac{100}{P_{\text{x,VSS}} + m_{\text{PS,VSS}}} \tag{27}$$

$$\eta_{\text{DIG,TSS}} = \left\{ \eta_{\text{DIG}} \cdot \left[\frac{Q \cdot \text{pCOD}_{\text{PI}} \cdot \eta_{\text{PS}}}{\text{pCOD/VSS}} + P_{\text{x, active bio}} \cdot \left(1 - f_{\text{d}} \right) \right] - 1.42 \cdot P_{\text{x,ANA}} \right\} \cdot \frac{100}{P_{\text{x,TSS}} + m_{\text{PS,VSS}}} \tag{28}$$

where

$\eta_{\text{DIG,VSS}}$ = VSS destruction in the digester (%)

$\eta_{\text{DIG,TSS}}$ = TSS reduction in the digester (%)

The balance in terms of COD units is a more detailed approach than the textbook-based VSS analysis:

$$m_{\text{BS,VSS}} = (Q \cdot \text{bVSS}_{\text{PS}} + Q \cdot \text{bVSS}_{\text{SS}}) \cdot (1 - \eta_{\text{DIG,VSS}}) \tag{29}$$

$$m_{\text{BG,VSS}} = (Q \cdot \text{bVSS}_{\text{PS}} + Q \cdot \text{bVSS}_{\text{SS}}) \cdot (\eta_{\text{DIG,VSS}}) \tag{30}$$

where

$m_{BS,VSS}$ = mass flow of biosolids calculated from VSS destruction (mass$_{VSS}$/d)

$m_{BG,VSS}$ = mass flow of biogas calculated from VSS destruction (mass$_{BG}$/d)

bVSS$_{PS}$ = biodegradable VSS in primary sludge (mass$_{VSS}$/d)

bVSS$_{SS}$ = biodegradable VSS in secondary sludge (mass$_{VSS}$/d)

$\eta_{DIG,VSS}$ = percent VSS destruction in the digester (%)

The percent VSS destruction in the digester $\eta_{DIG,VSS}$ is solely a function of the digester solid retention time SRT$_{dig}$ (d; Metcalf and Eddy, 2003), which makes no distinction of the nature of the influent VSS (e.g., primary sludge vs. secondary sludge and above all biodegradable vs. non-biodegradable). Hence, the specific biogas production (expressed in Nm^3/kgVSS$_{destroyed}$) is much more uncertain.

The relative performance in terms of bCOD transformation, bVSS and VSS destruction, TSS reduction, and COD of the supernatant for variable pCOD/VSS values are reported in Table 4.

2.3.4. Energy flow modelling

In Fig. 1 we also report the relationship between energy demand, energy requirements and the COD fractions.

Total energy demand e_D (kWh/d) is calculated as:

$$e_D = e_{D,PS} + e_{D,ASP} + e_{D,SS} + e_{D,AD} + e_{D,O} \tag{31}$$

where $e_{D,PS}$ = energy demand for primary sedimentation (kWh/d)

$e_{D,ASP}$ = energy demand for activated sludge aeration (kWh/d)

$e_{D,SS}$ = energy demand for secondary sedimentation (kWh/d)

$e_{D,AD}$ = energy demand for anaerobic digestion (kWh/d).

$e_{D,O}$ = energy demand for other equipment (kWh/d)

The energy demand e_D (kWh/d) of the process illustrated in Fig. 1 is dominated by the aeration energy for biological oxidation in the activated sludge process and details on the calculation of $e_{D,ASP}$ can be found in Monteith et al. (2005) and in Rosso and Stenstrom (2005) and according to values indicated in Table 3. The dominance of aeration energy on the overall process energy consumption was confirmed for the location where this model was tested. The other significant energy demanding process (digestion) mainly relies on waste heat and the values used in this paper are specific to the plant modelled here, and are again summarised in Table 3.

We excluded here influent and effluent pumping, since pumping is site-specific and coastal plants discharging against tidal cycles or plants injecting their effluent in deep aquifers or plants with deep sewers would be unfairly disadvantaged in the overall COD-based calculations. This is because pumping energy is calculated only on the basis of

hydraulic flow, regardless of the COD concentration. Also, the energy demand for effluent disinfection heavily depends on the disinfection modality (chemical with on-site chemical generation, chemical with purchase of disinfectant from an off-site location, or by irradiation) and is therefore site-specific. The actual calculation of energy demand adsorbs in e_O all other minor contributions assumed from literature and site-specific data (details on methodology published in Rosso and Stenstrom, 2005, 2008).

In this paper, we assume a fixed concentration of ammonia and TKN entering the plant, so that their effect on oxygen therefore energy demand is constant throughout our pCOD/VSS domain. The energy recovery e_R (kWh/d) from digester biogas is proportional to the biogas produced (Eq. (24)) which is in turn proportional to the removal of bCOD in the digester (Eqs. (22) and (23)):

$$e_R = \eta_{ER} \cdot h_{BG} \cdot m_{BG} \tag{32}$$

where

η_{ER} = efficiency of the energy recovery unit (−)

h_{BG} = calorific value of the biogas (kJ/kg$_{biogas}$)

2.3.5. Carbon footprint calculation

The following contributions to CO$_{2,eq}$ emission were considered: direct CO$_2$ emission from biological processes (ASP and AD); direct CO$_2$ emission from biogas combustion; indirect CO$_2$ emission from off-site power generation; CO$_{2,eq}$ offset from biogas energy recovery; CO$_{2,eq}$ emission due to CH$_4$ fugitive emission; CO$_{2,eq}$ emission due to CH$_4$ released during biosolids dewatering. The global warming potential for CH$_4$ was calculated at the 100 year horizon, i.e. 25 kg$_{CO_2eq}$/kg$_{CH_4}$ (IPCC, 2007). We quantify here only the carbonaceous emissions or emission equivalents from treatment, since the focus of this paper is the effects of COD fractional variations on carbon and energy footprint. N$_2$O has no effect on energy footprint and at the present moment there is no evidence linking COD fractional variations on varying N$_2$O emissions.

In the calculation of the CO$_2$ direct emission due to microbial respiration in ASP, it is important to highlight the carbon emission intensity of COD (i.e. the amount of CO$_2$ emitted per unit of COD oxidised, or κ_{COD}). In this study we hypothesised that wastewater organic compounds could be represented through the formula C$_{10}$H$_{19}$O$_3$N which is widely used for the case of domestic wastewater (inter alia, Monteith et al., 2005; Shahabadi et al., 2010). Considering the following oxidation reaction of the compound:

$$C_{10}H_{19}O_3N + 25/2O_2 \rightarrow 9CO_2 + NH_4^+ + HCO_3^- + 7H_2O \tag{33}$$

we obtain that $\kappa_{COD} = 0.99$ kg$_{CO_2eq}$/kg$_{COD}$. Analogously, in case of activated sludge biomass, considering the following stoichiometric relationships for biomass decay in aerobic environment:

$$C_5H_7O_2N + 5O_2 \rightarrow 4CO_2 + NH_4^+ + HCO_3^- + H_2O \tag{34}$$
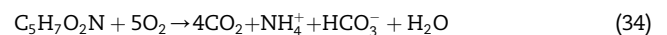
we obtain that $\kappa_{BIOMASS} = 1.03$ kg$_{CO_2eq}$/kg$_{COD}$. Both Eqs. (33) and (34) assume that the HCO$_3^-$ produced is in equilibrium in the liquid environment, i.e. it is not converted to H$_2$CO$_3$. In this way, we are able to evaluate the CO$_2$ emitted due to bacterial respiration as a function of MCRT, whose variations are in

Table 4 – Performance variation of the anaerobic digester in terms of bCOD, VSS, and TSS.		
pCOD/VSS (gCOD/gVSS)		1.07 → 1.87
bVSS destruction	%	84.9 → 86.9
VSS destruction	%	47.9 → 55.9
TSS reduction	%	37.1 → 45.8
COD transformation	%	44.1 → 36.6
COD in supernatant	mg/l	441 → 948

turn reflected on the amount of biomass that undergoes decay.

With the exception of CH_4 traces released in the activated sludge off-gas, the remaining bCOD not used for synthesis in the activated sludge reactor is oxidised to CO_2:

$$
\begin{aligned}
m_{CO_2,ASP} = {}& Q \cdot \kappa_{COD} \cdot (1 - Y_H) \cdot \eta_{ASP} \cdot bCOD \\
&+ Q \cdot \kappa_{BIOMASS} \cdot Y_H \cdot \eta_{ASP} \cdot bCOD \frac{k_{d,H} \cdot MCRT}{1 + k_{d,H} \cdot MCRT}(1 - f_d) \\
&- Q \cdot \kappa_{BIOMASS} \cdot Y_A \cdot \frac{NO_x}{1 + k_{d,A} \cdot MCRT} \\
&+ Q \cdot \kappa_{BIOMASS} \cdot Y_A \cdot NO_x \cdot \frac{k_{d,A} \cdot MCRT}{1 + k_{d,A} \cdot MCRT}(1 - f_d) \\
\simeq {}& Q \cdot \kappa_{COD} \cdot (1 - Y_H) \cdot \eta_{ASP} \cdot bCOD \\
&+ Q \cdot \kappa_{BIOMASS} \cdot Y_H \cdot \eta_{ASP} \cdot bCOD \frac{k_{d,H} \cdot MCRT}{1 + k_{d,H} \cdot MCRT}(1 - f_d)
\end{aligned}
$$

(35)

where

κ_{COD} = carbon emission intensity of COD (kg_{CO_2eq}/kg_{COD})

$\kappa_{BIOMASS}$ = carbon emission intensity of biomass (kg_{CO_2eq}/kg_{COD}).

The first term summed in Eq. (35) is the direct oxidation of influent bCOD, while the second term is the endogenous respiration of microbial biomass.

Direct CO_2 emission from AD is calculated as:

$$ m_{CO_2,AD} = \frac{m_{BG}}{\rho_{BG}} \cdot \rho_{CO_2} \cdot 0.35 $$

(36)

Direct CO_2 emission from biogas combustion is calculated according to the combustion reaction of methane:

$$ m_{CO_2,CH_4comb} = m_{BG} \cdot (1 - \eta_{FE}) \cdot \frac{44}{16} $$

(37)

where η_{FE} represents the methane fugitive emission (% of total methane produced). Here we assume that 100% of the methane entering the combustion chamber is fully combusted to CO_2, although if site-specific data were available an efficiency of methane oxidation during combustion (<100%) could be defined.

The indirect CO_2 emission from off-site power generation ($m_{CO_2,PG}$), is calculated on the basis of specific CO_2 emission per unit of energy generated in the region where the treatment plant is located (EIA, 2009) (see Table 3 for details) as:

$$ m_{CO_2eq,PG} = \kappa_{PG} \cdot e_D $$

(38)

The $CO_{2,eq}$ offset from biogas energy recovery ($m_{CO_2eq,offset}$) is calculated as:

$$ m_{CO_2eq,offset} = e_R \cdot \kappa_{PG} $$

(39)

An assumption must be made on the methane released through fugitive emission. This is a non-point source due to the extensive length of the spatially distributed network of pipes, valves, safety units, and appurtenances for biogas conveyance. Currently, most large scale biogas flow metres cannot measure flow with an error below 5%, and therefore a biogas mass in the percent range is always unaccounted for. We assumed here a 2% fugitive emission. Furthermore, depending on the sludge dewatering technology employed, some of the methane contained in the biogas-saturated biosolids to dewater may be released directly to the atmosphere. This is the case of belt-press facilities, such as the one

performing sludge dewatering in this case, and we assumed that half of the methane contained in the biosolids is released during dewatering, and the other half is returned to biological oxidation where it ultimately becomes CO_2 with negligible contribution to the total CO_2 from influent bCOD oxidation emitted in the off-gas. Hence, the $CO_{2,eq}$ emission due to CH_4 fugitive emission ($m_{CH_4eq,fugitive}$) and to CH_4 released during biosolids dewatering ($m_{CH_4,dewatering}$) is calculated as:

$$ m_{CO_2eq,fugitive} = 25 \cdot \left(m_{CH_4,fugitive} \cdot \eta_{FE} + m_{CH_4,dewatering} \right) $$

(40)

Finally, total $CO_{2,eq}$ emission (kg_{CO_2eq}/d) is calculated as the sum of all contributions:

$$
\begin{aligned}
m_{CO_2eq} = {}& m_{CO_2,ASP} + m_{CO_2,AD} + m_{CO_2,CH_4comb} + m_{CO_2eq,PG} \\
&- m_{CO_2eq,offset} + m_{CO_2eq,fugitive}
\end{aligned}
$$

(41)

Both CFP and eFP are normalised per unit bCOD removed from the wastewater ($kg_{CO_2eq}/kg_{bCOD,rem}$ and $kWh/kg_{bCOD,rem}$, respectively) and per unit volume of treated wastewater ($kg_{CO_2eq}/m^3_{ww,treated}$ and $kWh/m^3_{ww,treated}$, respectively).

2.4. Model domain

Previously, several publications reported ranges of pCOD/VSS ratios (e.g. Takacs and Vanrolleghem, 2006). These ranges span over what we refer here as a range of possible pCOD/VSS values (from 1.07 to 2.87 gCOD/gVSS, for pure carbohydrates and pure lipids, respectively). By utilising our procedure for COD fractions calculation, the range of possible pCOD/VSS reported by Takacs and Vanrolloghem produces a number of unacceptable COD fractions (defined as sCOD < 0). The procedure fails (100% of fractions with sCOD < 0) with pCOD/VSS higher than 2.59 gCOD/gVSS. This is because very high values of pCOD/VSS, more representative of pure lipids, are unrealistic for a municipal wastewater.

In IWA (2008), Henze and Comeau report the typical composition of raw municipal wastewater with minor contribution of industrial wastewaters. Their values, used here as the most probable range, lead to pCOD/VSS in the range 1.22–1.50 gCOD/gVSS (corresponding to sCOD/COD of 0.40–0.26, respectively). On the other hand, in the literature review discussed by Ekama (2009), when the same value of pCOD/VSS is assumed for biodegradable and non-biodegradable particulate organics, pCOD/VSS spans over 1.40–1.62 gCOD/gVSS for primary sludge and over 1.32–1.57 and 1.19–2.17 for biodegradable and non-biodegradable particulate organics, respectively. Based on these sources we selected a pCOD/VSS domain of 1.07–1.87. This corresponds to 26.2% unacceptable COD fractions (i.e., sCOD < 0), which are excluded. These correspond to the influent conditions not usual for regular operations (e.g., during and immediately following storm events, during and immediately following holidays, sampling errors, etc.). The use of input data smoothing or averaging would reduce short-term fluctuations and highlight longer-term trends or cycles, thus reducing the amount of unacceptable COD fractions. On the other hand, this would protract the irregularities of short-term phenomena over the time-averaged period. In this research we do not aim at modelling COD fractions dynamically but

rather at developing a simplified approach for modelling the process energy in terms of COD fractions. Thus, our aim in defining the model domain is to reduce the effects of the inevitable plant data variation.

3.   Results and discussion

We analysed process data sets and produced yearly averages, reported in Fig. 2. The average coefficient of variation for the COD fractions in primary influent and effluent was 0.37 and 0.40, respectively. When calculating the average coefficient of variation for secondary effluent fractions, its value exceed 1.0 due to the substantial decrease of S_S and X_I. The COD, VSS and TSS removal during primary settling, calculated using plant data, equals 47.5%, 67.1% and 66.3%, respectively. Assuming a 66.7% VSS and TSS removal, and using our procedure, within the pCOD/VSS domain range, the COD removal in primary settling would span between 35% and 54%. The actual (i.e., based on plant data) and estimated (i.e., based on our procedure) COD removal in primary settling match when pCOD/VSS equals 1.57 gCOD/gVSS.

In Fig. 2, one can notice the expected relative increase in S_S (i.e., sbCOD) after primary settling, due to the decreased relative amount of particulate COD after a successful primary sedimentation. Even though the fractions reduce in absolute terms, when pCOD/VSS increases (Fig. 2, right panel) the relative increase in S_S (i.e., sCOD) is maximum. Due to its conservative nature, S_I always dominates the secondary effluent fraction, followed by X_S which is associated with the fraction of activated sludge biomass that does not settle well and is released from the secondary clarifiers. Since the process energy demand is largely dominated by the ASP energy (Reardon, 1995; Rosso and Stenstrom, 2005), in all cases within the pCOD/VSS range the reduction of S_S from primary effluent to secondary effluent is largely associated with the aeration energy demand for secondary oxidation. Conversely, since the energy recovery is associated with the solids flow to

the digester, even though the relative ratios of X_S along the process train appear to be similar for all the pCOD/VSS cases, the absolute value of digestible solids sent to the digesters increases with increasing pCOD/VSS, thereby increasing the energy recovery of the process. In sum, with higher pCOD/VSS (hence, with lower sCOD/COD), the process energy demand is decreased and its energy recovery increased, with compounding beneficial effect (highlighted in Figs. 3 and 4).

We report our process modelling results in terms of both mass of CO_2 equivalent emitted per unit bCOD removed ($kg_{CO_2eq}/kg_{bCODremoved}$) and per unit volume of wastewater treated ($kg_{CO_2eq}/m^3_{ww,treated}$). Both normalisations are valuable and have different significance, although in our results they overlap since we do not vary the average wastewater concentration. Reporting carbon equivalent emission per unit bCOD is the theoretical calculation of the global warming potential of the wastewater, since the alternative of no treatment at all would still yield a carbon equivalent emission (untreated bCOD is typically assumed to eventually become 50% CO_2 and 50% CH_4), beside the obvious public and environmental health threats associated with the untreated sewage discharge (Rosso and Stenstrom, 2008). The other output normalisation (i.e. $kg_{CO_2eq}/m^3_{ww,treated}$) is a measure of the site-specific carbon footprint of a process, as it implicitly includes information on the wastewater concentration. The two normalised measures are linearly scalable once the concentration of the influent wastewater is not varied, such as in our case. When dynamic modelling is practiced, the conversion of one normalisation to the other would follow the dynamic wastewater concentration curves. Finally, we choose here to omit the results in terms of absolute values of CO_2 mass flows (i.e., kg_{CO_2eq}/d), for these are highly site- and assumption- specific and have little or no value for modelling research, but are useful for emission reporting and process performance benchmarking, both outside the scope of this research.

Fig. 3 shows the carbon equivalent emission for the CFP contributions, expressed as $kg_{CO_2eq}/kg_{bCODremoved}$ and
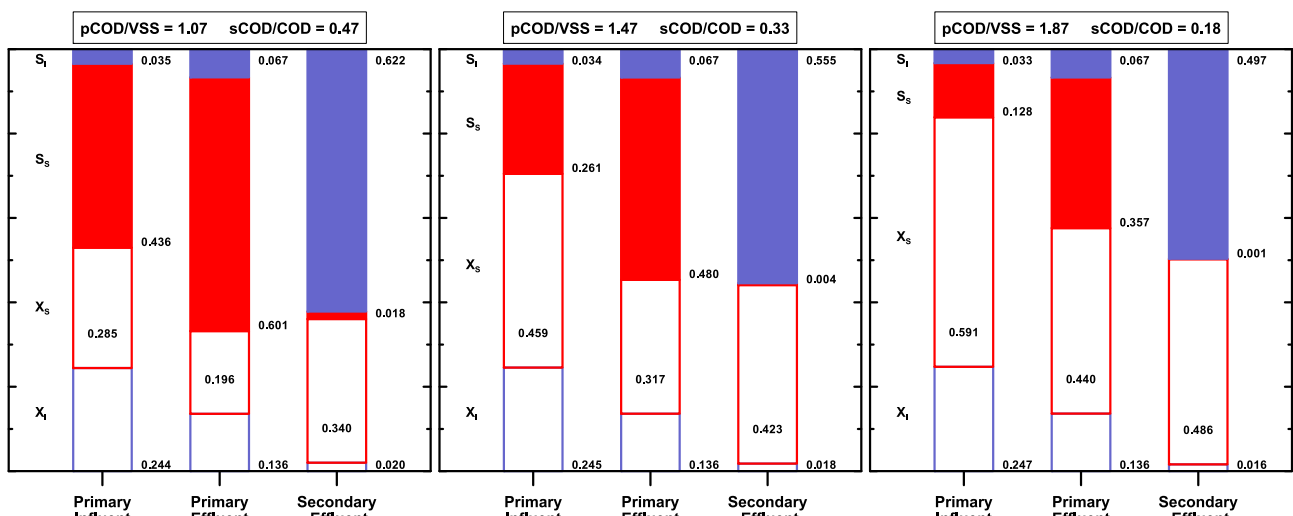

Fig. 2 – COD fractions from the case plant considered for increasing pCOD/VSS ratios (average of 365 days for each panel; cases with negative sCOD excluded).
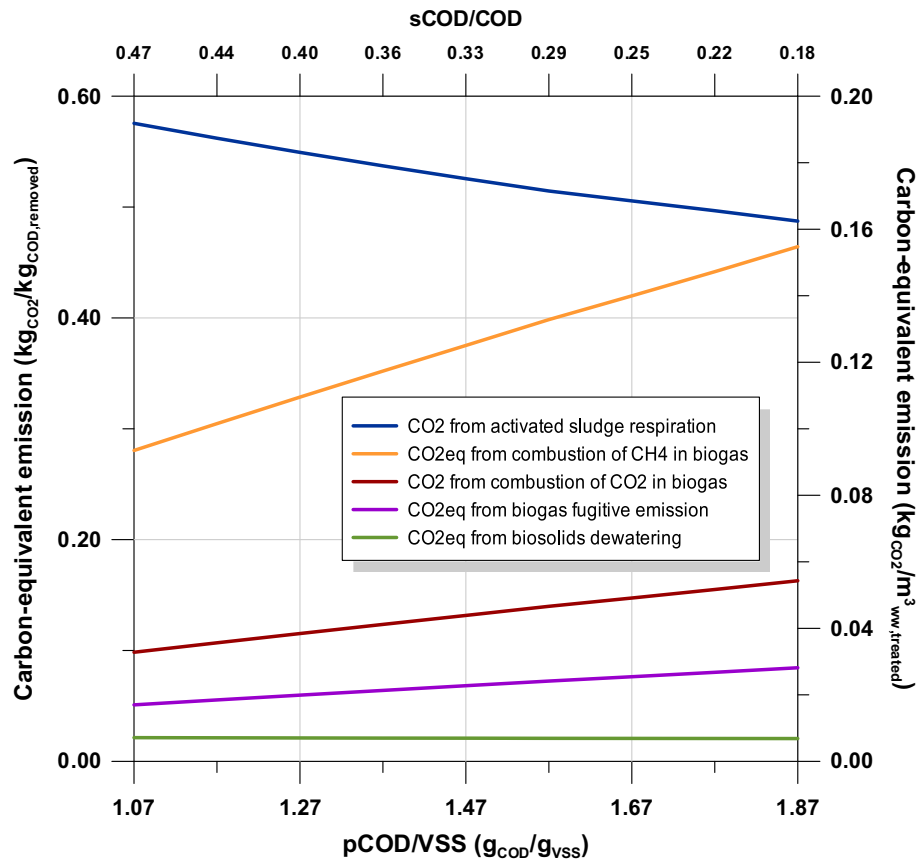
Fig. 3 − Carbon footprint components (expressed as $kg_{CO_2eq}/kg_{bCODremoved}$ and as $kg_{CO_2eq}/m^3_{ww,treated}$) against varying pCOD/VSS and sCOD/COD ratios.

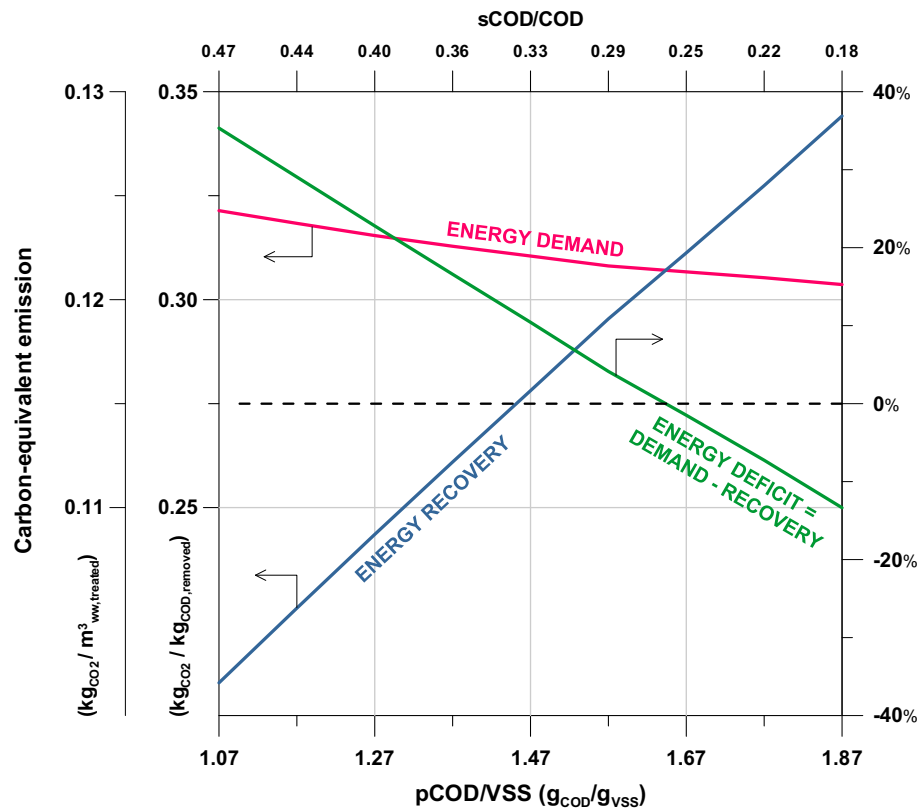**Fig. 4 − Energy footprint components, and energy deficit for varying pCOD/VSS and sCOD/COD ratios.**

$kg_{CO_2eq}/m^3_{ww,treated}$ against varying pCOD/VSS and sCOD/COD ratios. Higher particulate in the influent implies higher removal of bCOD in the primary settler (affecting all but the blue line in Fig. 3), which results in lower CO_2 emitted by bacterial respiration (blue line). This also implies lower activated sludge biomass production, which increases the fraction of sludge from primaries in the digester's influent, yielding more methane and proportionally lower biosolids mass for disposal.

The same discussion is applicable to Fig. 4, where the energy demand, recovery, and deficit are plotted for varying pCOD/VSS and sCOD/COD values. In this graph, as the fraction of sCOD decreases, the energy burden to the aeration system decreases, in turn driving down the overall process energy demand. Concurrently, the particulate fraction of the COD increases, thereby increasing the solids load to the digester and its biogas production. The energy recovery then increases, and the process energy balance shifts from a net energy deficit at low pCOD/VSS (i.e., high sCOD/COD) to a net energy recovery at high pCOD/VSS (i.e., low sCOD/COD). The energy demand and recovery trends in Fig. 4 may appear discrepant, but it must be remembered that when the bCOD is treated in the secondary rather than the primary, its fate is both respiration corresponding to a net energy demand, and synthesis corresponding to a partial energy recovery through biomass digestion. But since not all VSS are equally digestible (in fact pCOD/VSS for primary sludge span over 1.07—1.87 while is constant at 1.42 g_{bCOD}/g_{VSS} for the activated sludge biomass), by treating more bCOD in the secondary treatment the process shifts its energy balance from high recovery to much higher demand, in proportion. Hence, the different slopes of energy demand and recovery in Fig. 4. The energy deficit shifts at a certain pCOD/VSS value, showing that process energy self-sufficiency may be possible, as demonstrated by Wett et al. (2007), although unlike the case of Wett et al. (2007) most processes are fully aerobic (i.e., with higher energy requirements) and wastewaters could be in the lower range of pCOD/VSS and therefore seldom able to yield sufficient energy to fully offset the energy demand, as discussed by Ekama (2009). Also, the energy recovery is calculated assuming an efficiency for the energy recovery process. This varies amongst energy recovery processes (e.g., combined heat and power generation, fuel cells, mechanical engines, etc.) and for large installations could be as efficient as 33—40% as electrical energy recovery and 48—50% as thermal energy recovery (Pöschl et al., 2010). Combined energy recovery (i.e., electrical plus thermal) up to 60% is possible (IWA, 2008). In case of warm climates the waste heat may be excessive and only partially recovered, therefore the combined energy recovery may be lower than 60%, hence our assumption of 50% energy recovery for this process. Nevertheless, in cold weather facilities the waste heat from co-generation may not be sufficient and energy importation (e.g., as supplemental natural gas purchase) may be required.

We present the results of the model sensitivity analysis in the graphs in Fig. 5 and in Table 5. The relative behaviour of the parameter variation in the pCOD/VSS range confirms the results reported above. CO_2 emission from respiration decreases with pCOD/VSS increasing. This is due to a decreased fraction of soluble substrate to be biologically
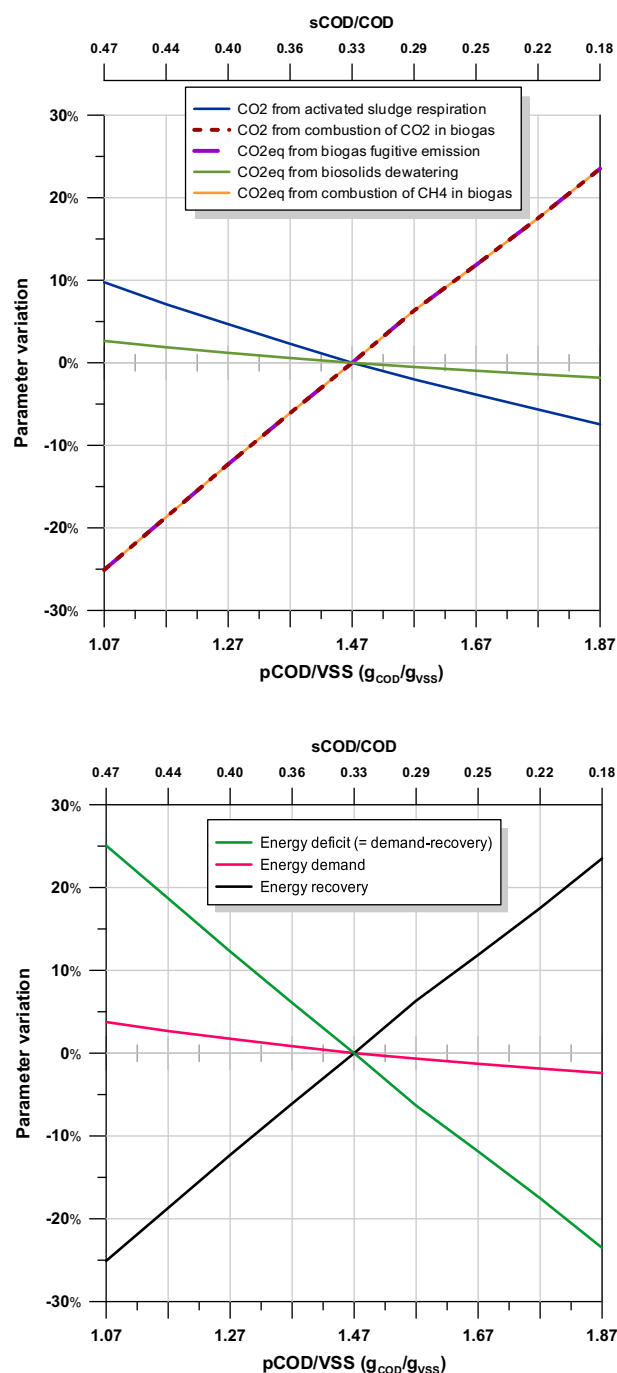

Fig. 5 — Sensitivity charts.

oxidised in the aeration tank. At the same time, the energy demand increases with decreasing pCOD/VSS ratio due to the higher fraction of soluble material to be biologically oxidised in the aeration tank. Being aeration the largest contributor to power consumption, the overall power consumption is driven upwards. The energy recovery increases with increasing pCOD/VSS ratio, due to the higher solids fraction sent to digestion directly from primary sedimentation. Coupled with the associated decrease in soluble matter to be biologically oxidised, an increased pCOD/VSS ratio leads to overall decreased net energy usage and lowering energy deficit.

Table 5 – Summary of sensitivity analysis.										
pCOD/VSS (gCOD/gVSS) →		1.07	1.17	1.27	1.37	1.47	1.57	1.67	1.77	1.87
Variation of:										
CO_2 from respiration	%	25.23	18.40	12.04	5.89	0.00	−5.45	−10.03	−14.57	−19.26
CO_2 in biogas	%	−24.18	−18.06	−11.89	−5.90	0.00	6.18	11.64	17.25	23.18
CO_{2eq} from biogas CH_4 combustion	%	−24.18	−18.06	−11.89	−5.90	0.00	6.18	11.64	17.25	23.18
CO_{2eq} of biogas fugitive emissions	%	−24.18	−18.06	−11.89	−5.90	0.00	6.18	11.64	17.25	23.18
CO_{2eq} of CH_4 emission during sludge dewatering	%	4.08	2.93	1.88	0.91	0.00	−0.83	−1.53	−2.21	−2.89
CO_{2eq} of N_2O emission from activated sludge	%	0.00	0.00	0.00	0.00	0.00	0.00	0.00	0.00	0.00
CO_{2eq} of energy demand	%	10.16	7.35	4.78	2.32	0.00	−2.08	−3.81	−5.49	−7.22
CO_{2eq} of energy recovery	%	−24.18	−18.06	−11.89	−5.90	0.00	6.18	11.64	17.25	23.18

Biogas production decreases with decreasing pCOD/VSS ratio, due to the decreased particulate fraction sent to digestion from primary sedimentation and to slightly increased soluble substrate available to activated sludge synthesis. Along with biogas production, its fugitive emission, here quantified as a percent of biogas production, decreases with the same trend. Biogas emission during dewatering, however, decreases by a lesser extent because of the varying biogas yield (expressed as $Nm^3_{biogas}/kg_{VSS,destroyed}$) due to varying composition of primary vs. secondary sludge in the digester influent.

Our analysis cannot distinguish, at this moment, the different weight that regional practices, such as disposing of food waste in sewers, or site-specific operations, such as the addition of coagulants to primary sedimentation, could have on the modelling results. Food waste disposal in wastewater, which could be presented as a carbon footprint mitigation factor (Evans, 2009), is typical in the United States. Other areas of the world with moderate or no disposal of food waste in sewers would be expected to have not only lower TSS and VSS values in their influent, but also different pCOD/VSS ratios. These would not necessarily be lower, as food waste is largely composed of cellulosic matter, which is in the lower range of pCOD/VSS, according to Takacs and Vanrolleghem (2006). Also, the practice of source-separation of fats, oil and grease (FOG), especially for commercial establishments such as restaurants or communal kitchens, and its diversion to digestion via collection programs, offers the opportunity for increased biogas generation and for sheltering the activated sludge from the elevated energy requirements associated with FOG oxidation. Since FOG is a "rich" VSS component (i.e., very high pCOD/VSS ratio according to Takacs and Vanrolleghem, 2006), the expectable biogas yield in the digester could be higher, in proportion.

In the case of industrial wastewater treatment plants, the pCOD/VSS ratios would be skewed by sector, but the model structure would not need modification. For example, a ratio of pCOD/VSS close to 1.07 is characteristic of wastewater rich in carbohydrates such as winery or brewery wastewater, and previous CFP modelling (e.g. Rosso and Bolzonella, 2009) could be further refined by introducing the current approach on COD fractions.

This model offers a rigorous tool to evaluate the effect of variations in primary treatment on the process eFP and CFP. For example, this model can be used to quantify the eFP and CFP effects and the associated costs vs. the benefits of enhancing the removal of sludge in the primary treatment via the aid of coagulants. Certainly, the addition of a coagulant to enhance primary sedimentation, despite its operating cost, would be expected to relieve the activated sludge from part of the load which in turn would be sent to digestion, with higher energy recovery. The energy deficit would be expected to decrease, but more often than not the choice of adding coagulants is driven by either land constraints for sedimentation expansion or need to sequester sulphides to curb odorous release. In this case, the ratio of pCOD/VSS in the primary effluent would be different than in the case of no coagulant added, and the model should be adapted accordingly. The opportunity to effectively enhance primary sedimentation must be also analysed under the point of view of incidental enhanced removal of the fraction of bCOD (i.e., rbCOD) that favours denitrification, hence BNR. Nutrient removal could suffer in case of wastewater with low C/N and C/P ratios (Puig et al., 2010) and extended MCRT to achieve nutrient removal in activated sludge may be required. Further research should address the effects of differential removal of COD fractions during enhanced primary sedimentation on the effectiveness of nutrient removal.

The temporal variability in data input and its reflection on the COD fractions and on the model domain discussed in the methodology should be the object of future research. Using a moving average of the influent data to smoothen the effects of short-term irregularities would highlight longer-term trends and seasonal cycles. For example, one here should argue that the temperature of the influent wastewater and the hydraulic residence time in the sewer network have an effect on the influent sCOD/COD ratio, thereby on pCOD/VSS. That is expected to be true, due to higher rate of substrate hydrolysis and consequently methanogenesis at warmer temperature and longer residence time (Guisasola et al., 2008). The plant we modelled here is located in an area with warm wastewater throughout the year where major seasonal variations could not be detected. Another plant with four seasons and a substantial difference in wastewater temperature over the yearly cycle would be expected to exhibit different behaviour. Also, in our modelling we do not currently compare plants fed by sewers of different length or by combined sanitary and storm sewers. Sewer length would have an effect on the sCOD/COD ratio, especially at higher wastewater temperatures where sewers act in effect as plug flow reactors for hydrolysis (Guisasola et al., 2008). In any case, our model begins calculating the COD fractions at the plant influent well, and is hence independent of the in-sewer processes. However, due to different sewer geometry and sewage characteristics,

a plant could have different influent fractions for same sewage or similar fractions for different sewage, respectively. Future research efforts should address these two sensitive components.

Also, future research should investigate the effects of varying NOD/TOD for a given pCOD/VSS ratio, as temperature and sewer length would affect the release of ammonia from organic nitrogen. The ammonia released in the sewer is treated in the secondary process, thereby increasing even further the energy burden on the aeration system. Colder wastewaters and shorter sewer lines could be expected to have an advantage, as the organic nitrogen still embedded in the solids would be sent to digestion instead of secondary nitrification/denitrification. This would be of no consequence in the (usual) case of supernatant return to the head of the primary treatment. Therefore, in our current modelling work we did not consider variable ammonia values, since the supernatant here is fully returned to the headworks. However, as alternative low energy footprint options for side-stream treatment of highly rich nitrogen flows (such as digesters' supernatant) become available [e.g., the simultaneous chemical precipitation of nitrogen with magnesium ammonium salts (Schultze-Rettmer, 1991; Zdybiewska and Kula, 1991), or biological treatment with anaerobic or microaerophilic processes (e.g., Siegrist, 1996; van Dongen et al., 2001; Fux et al., 2003; Wett, 2007)], they should also be considered for reducing the overall process energy and carbon footprint by relieving the main biological process form loading shocks and energy peaks.

This model does not aim at replacing the full-featured process models (e.g., ASM, ADM) but introduces a simplified methodology that relies on the restricted data sets typically available for most treatment plants. The next logical step should be the plant-wide integration of the full-featured process models and their extension to include the energy and carbon footprint components.

4.   Conclusions

We analysed in this paper the different effects of COD fractions on carbon and energy footprint of a wastewater treatment process using activated sludge with nutrient removal and anaerobic sludge digestion with biogas energy recovery. Also, we introduce a simplified procedure to evaluate COD fractions using process parameters typically collected in plants (e.g., VSS, BOD_5, etc.) and assuming a pCOD/VSS value. A real municipal wastewater treatment process was modelled with this procedure and the results for energy and carbon footprint, as direct and indirect emissions, are reported here.

Our results show that the ratio sCOD/COD may alter the carbon and energy footprint of a process, as it dictates where the COD is processed: either recovering energy after biogas production in a digester, or demanding energy for aerobic oxidation in the activated sludge reactor. For a given process, the increase of the ratio sCOD/COD increases the process carbon and energy footprint. Conversely, an increase in particulate (e.g., pCOD/COD) removed in the primary sedimentation would reduce the energy demand on the aeration

reactors and the associated CO_2 direct emission from respiration and indirect emission for power generation. Even though the apparent conclusion is to promote primary sedimentation, care must be used during process analysis since a fraction of the COD necessary for proper nutrient removal downstream may be incidentally removed.

REFERENCES

Ahn, J.H., Kim, S., Park, H., Rahm, B., Pagilla, K., Chandran, K., 2010. N_2O emissions from activated sludge processes, 2008–2009: results of a national monitoring survey in the United States. Environ. Sci. Technol. 44, 4505–4511.

de Haas, D., Foley, J. and Barr, K., 2008. Greenhouse gas inventories from WWTPs – The trade-off with nutrient removal. Proc. Water Environment Federation Sustainability Conference, National Harbour, MD.

EIA - United States Energy Information administration, 2009. Annual Energy Outlook 2009 – With projections to 2030 DOE/EIA-0383(2009), Washington, DC.

Ekama, G.A., 2009. Using bioprocess stoichiometry to build a plant-wide mass balance based steady-state WWTP model. Wat. Res. 43 (8), 2101–2120.

Evans, T.D., 2009. Climate change impacts of food waste diversion to anaerobic digesters. Proc. 23rd Water Environment Federation, Annual Residuals & Biosolids Conference, 1056–1076, Portland OR.

Foley, J., de Haas, D., Hartley, K., Lant, P., 2010. Comprehensive life cycle inventories of alternative wastewater treatment systems. Wat. Res. 44 (5), 1654–1666.

Fux, C., Lange, K., Huber, P., Grueniger, B., Siegrist, H., 2003. Nitrogen removal from digester supernatant via nitrite – SBR or SHARON? Wat. Sci. Technol. 48 (8), 9–18.

Grady, L.C.P., Daigger, G.T., Lim, H.C., 1998. Biological Wastewater Treatment, second ed. CRC Press, New York.

Guisasola, A., de Haas, D., Keller, J., Yuan, Z., 2008. Methane formation in sewer systems. Wat. Res. 42 (6–7), 1421–1430.

Henze, M., 1992. Characterization of wastewater for modelling of activated sludge processes. Wat. Sci. Technol. 35 (9), 113–120.

Henze, M., Grady, C.P.L., Gujer, W., Marais, G.v.R., Matsuo, T., 1987. Activated Sludge Model No. 1. Scientific and Technical Report No. 1. IAWPRC, London.

Henze, M., Gujer, W., Mino, T., van Loosdrecht, M.C.M., 2000. Activated Sludge.

Hulsbeek, J.J.W., Kruit, J., Roeleveld, P.J., van Loosdrecht, M.C.M., 2002. A practical protocol for dynamic modelling of activated sludge systems. Wat. Sci. Technol. 45 (6), 127–136.

IPCC, 2007. Climate change 2007: the physical science basis. In: Solomon, S., Qin, D., Manning, M., Chen, Z., Marquis, M., Averyt, K.B., Tignor, M., Miller, H.L. (Eds.), Contribution of Working Group I to the Fourth Assessment Report of the Intergovernmental Panel on Climate Change. Cambridge University Press, Cambridge, NY, p. 996.

IWA, 2008. Biological Wastewater Treatment – Principles, Modelling and Design. IWA Publishing.

Metcalf, & Eddy, Inc, 2003. Wastewater engineering: treatment and reuse. In: Tchobanoglous, G., Burton, F.L., Stensel, H.D. (Eds.), McGraw-Hill Series in Civil and Environmental Engineering, fourth ed. (New York).

Metcalf, L., Eddy, H.P., 1914. American Sewerage Practice, first ed. McGraw-Hill, New York.

Monteith, H.D., Sahely, H.R., MacLean, H.L., Bagley, D.M., 2005. A rational procedure for estimation of greenhouse-gas emissions from municipal wastewater treatment plants. Wat. Environ. Res. 77, 390–403.

Models ASM1, ASM2, ASM2d, and ASM3. Scientific and Technical Report n. 9. IWA Publ., London.

Pöschl, M., Ward, S., Owende, P., 2010. Evaluation of energy efficiency of various biogas production and utilization pathways. Appl. Energy 87 (11), 3305–3321.

Park, H.D., Lee, Y.H., Kim, H.B., Moon, J., Ahn, C.H., Kim, K.T., Kang, M.S., 2010. Reduction of membrane fouling by simultaneous upward and downward air sparging in a pilot-scale submerged membrane bioreactor treating municipal wastewater. Desalination 251 (1–3), 75–82.

Puig, S., van Loosdrecht, M.C.M., Flameling, A.G., Colprim, J., Meijer, S.C.F., 2010. The effect of primary sedimentation on full-scale WWTP nutrient removal performance. Wat. Res. 44 (11), 3375–3384.

Reardon, D.J., 1995. Turning down the power. Civ. Eng. 65 (8), 54–56.

Roeleveld, P.J., van Loosdrecht, M.C.M., 2002. Experience with guidelines for wastewater characterisation in the Netherlands. Wat. Sci. Technol. 45 (6), 77–87.

Rosso, D., Bolzonella, D., 2009. Carbon footprint of aerobic winery wastewater treatment. Wat. Sci. Technol. 60 (5), 1185–1189.

Rosso, D., Stenstrom, M.K., 2005. Comparative economic analysis of the impacts of mean cell retention time and denitrification on aeration systems. Wat. Res. 39 (16), 3773–3780.

Rosso, D., Stenstrom, M.K., 2008. The carbon-sequestration potential of municipal wastewater treatment. Chemosphere 70, 1468–1475.

Rosso, D., Desai, A.S., Tseng, L.Y., 2009 Effects of nitrous oxide emissions on process carbon footprint of wastewater treatment plants, Proc. 2nd IWA BNR Conf., Krakow, Poland.

Schultze-Rettmer, R., 1991. The simultaneous chemical precipitation of ammonium and phosphate in the form of magnesium-ammonium-phosphate. Wat. Sci. Technol. 23, 659–667.

Shahabadi, B.M., Yerushalmi, L., Haghighat, F., 2010. Estimation of greenhouse gas generation in wastewater treatment plants – Model development and application. Chemosphere 78, 1085–1092.

Siegrist, H., 1996. Nitrogen removal from digester supernatant – Comparison of chemical and biological Methods. Wat. Sci. Technol. 34 (1–2), 399–406.

Takacs, I. and Vanrolleghem P.A., 2006. Elemental balances in activated sludge modelling. Proc. of the IWA World Water Congress, 10–14 September 2006, China.

van Dongen, U., Jetten, M.S.M., van Loosdrecht, M.C.M., 2001. The SHARON®-Anammox® process for treatment of ammonium rich wastewater. Wat. Sci. Technol. 44 (1), 153–160.

Vanrolleghem, P.A., Insel, G., Petersen, B., Sin, G., De Pauw, D., Nopens, I., Weijers, S. and Gernaey, K., 2003. A comprehensive model calibration procedure for activated sludge models. Proc. of WEFTEC 76th Annual Technical Exhibition and Conference, October 11–15, Los Angeles, California.

Vollertsen, J., Almeida, M.d.C., Hvitved-Jacobsen, T., 1999. Effects of temperature and dissolved oxygen on hydrolysis of sewer solids. Wat. Res. 33 (14), 3119–3126.

Wett, B., 2007. Development and implementation of a robust deammonification process. Wat. Sci. Technol. 56 (7), 81–88.

Wett, B., Buchauer, K. and Fimml, C., 2007. Energy self-sufficiency as a feasible concept for wastewater treatment systems. Proc. IWA LET Conf., Singapore. Asian Water, 09/07, 21–24.

Zdybiewska, M.W., Kula, B., 1991. Removal of ammonia nitrogen by the precipitation method, on the example of some selected waste waters. Wat. Sci. Technol. 24 (7), 229–234.